LA-UR-02-5700

Approved for public release;
distribution is unlimited.

Title: Autocorrelation and Dominance Ratio in Monte Carlo Criticality Calculations

Author(s): Taro Ueki, Forrest B. Brown, D. Kent Parsons, Drew E. Kornreich

Submitted to: Nuclear Science & Engineering journal, American Nuclear Society

Autocorrelation and Dominance Ratio in Monte Carlo Criticality Calculations

Taro Ueki and Forrest B. Brown

Diagnostics Applications Group (X-5), Applied Physics Division,

D. Kent Parsons

Primary Design & Assessment Group (X-4), Applied Physics Division,

and

Drew E. Kornreigh

Technology Modeling & Analysis Group (D-7), Decision Applications Division

Los Alamos National Laboratory

Send Correspondence to:

Taro Ueki
PO Box 1663, MS F663
Los Alamos, NM 87545
Email: ueki@lanl.gov
Phone: 505-665-0813
Fax: 505-665-3046

ABSTRACT

The iteration cycle-to-cycle correlation (autocorrelation) in Monte Carlo (MC) criticality calculations is analyzed concerning the dominance ratio of fission kernels. The mathematical analysis focuses on how the eigenfunctions of a fission kernel decay if operated on by the cycle-to-cycle error propagation operator of the MC stationary source. The analytical results obtained can be summarized as follows: When the dominance ratio of a fission kernel is close to unity, the autocorrelation of the tallies of the neutron effective multiplication factor is not strong and may be negligible, while the autocorrelation of the MC stationary source is strong and decays slowly. The practical implication is that when one analyzes a critical reactor with a large dominance ratio, the MC confidence interval estimation of quantities like the fission rate at individual locations must account for the strong autocorrelation. Numerical results are presented for sample problems with a dominance ratio of 0.85-0.99, where Shannon and relative entropies are utilized to exclude the influence of initial nonstationarity.

I. INTRODUCTION

It has been argued in the MC criticality analysis community that the tallies of a neutron effective multiplication factor (k_{eff}) from stationary source iteration cycles are directly related to the dominance ratio of fission kernels.[1] It is also widely accepted that the larger the dominance ratio is, the stronger the autocorrelation of the MC stationary source is. Recent work[2] has shown that when the immediate importance, i.e., importance to the first generation descendent particles, is spatially flat, the autocorrelation of the k_{eff} tallies is negligible. This appears to yield contradictory conclusions because in large homogeneous reactors the dominance ratio may be close to unity and the immediate importance is nearly flat except in the peripheral regions. What is wrong in the above arguments? Here, one can easily notice that a distinction between the stationary source distribution and its integrated quantities is missing. In this paper, the effect of dominance ratio on autocorrelation is analyzed concerning the fission source at individual spatial locations and k_{eff}, the integral of the source over the whole fissile domain. The effect of symmetry is also investigated in terms of the location of spatial binning. Mathematical analysis is performed within the framework of the fission site generation and k_{eff} estimator of absorption and collision types. Numerical results are presented for sample problems with a dominance ratio of 0.85-0.99, where great care is taken to exclude the influence of initial nonstationarity using the Shannon and relative entropies[3] of MC source.

II. RANDOM NOISE PROPAGATION IN STATIONARY CYCLES

Let $F(\vec{r}' \to \vec{r})$ be the expected number of the first generation descendant particles per unit volume at $\vec{r}$ resulting from a particle born at $\vec{r}'$. In the case of a position independent

energy spectrum, $F(\vec{r}' \to \vec{r})$ is the fission kernel defined by the product of energy and angular spectrums, an inverse transport operator and a fission operator in that order (from right to left) with the last operator defined as $\int\int \nu\Sigma_f(\vec{r},E)\psi(\vec{r},E,\vec{\Omega})d\Omega dE$ for the operand ψ and the fissile descendent generation cross section $\nu\Sigma_f$. The eigenfunction and eigenvalue of F are denoted by S_j and k_j:

$$S_j(\vec{r}) = \frac{1}{k_j}\int S_j(\vec{r}')F(\vec{r}' \to \vec{r})dr', \tag{1}$$

where k_j are ordered as $k_0 > |k_1| > |k_2| > \cdots$. As in previous work[1], the eigenvalue k_j's are assumed to be discrete. Note that k_{eff} is the largest eigenvalue k_0 and S_0 is called the fundamental mode eigenfunction and assumed to be normalized to k_0:

$$\int S_0(\vec{r})dr = k_0 . \tag{2}$$

The normalization condition (2) cannot generally be assuemed for S_j, $j \geq 1$ because in symmetric problems eigenfunctions may integrate to zero for some of the non-fundamental modes. In order to simplify later derivations, the following condition is imposed on the nonfundamental mode eigenfunctions:

$$S_j(\vec{r}) \leftarrow \frac{k_j S_j(\vec{r})}{\int S_j(\vec{r})dr} \text{ when } \int S_j(\vec{r})dr \neq 0 , \tag{3}$$

i.e., the whole domain integral of $S_j(\vec{r})$ is normalized to the corresponding eigenvalue as far as $\int S_j(\vec{r})dr \neq 0$ and no specification is made otherwise. The source (distribution of fission sites) after simulating the m-th stationary cycle in a MC criticality calculation is written as

$$\hat{S}^{(m)}(\vec{r}) = NS(\vec{r}) + \sqrt{N}\hat{e}^{(m)}(\vec{r}), m \geq 0 , \tag{4}$$

where $\hat{e}^{(m)}(\vec{r})$ is the fluctuating component of the stationary source, N the number of particle histories per cycle, the hats indicate a realization of stochastic quantities, and $S(\vec{r})$ is the expected value (ensemble average) of $\hat{S}^{(m)}(\vec{r})/N$:

$$S(\vec{r}) = \frac{1}{N} E\left[\hat{S}^{(m)}(\vec{r})\right]. \tag{5}$$

Note that Eq. (5) implies $E[\hat{e}^{(m)}(\vec{r})] = 0$. The scaling by N and $\sqrt{N}$ in (4) is based on the random nature of individual particle tracking processes. In other words, the relative fluctuation of particle population $\int\left[\hat{S}^{(m)}(\vec{r}) - E[\hat{S}^{(m)}(\vec{r})]\right]dr \Big/ \int E[\hat{S}^{(m)}(\vec{r})]dr$ can be scaled by the inverse of the square root of population when the population is sufficiently large. In addition, the number of particle histories is assumed to be fixed throughout cycles. The bias of $S(\vec{r})$ is of order $1/N$ for discretized[4] and continuous[5] models:

$$S(\vec{r}) - S_0(\vec{r}) = \mathrm{O}(1/N). \tag{6}$$

The explicit form of $\hat{S}^{(m)}(\vec{r})$ is

$$\hat{S}^{(m)}(\vec{r}) = \sum_{i=1}^{I(m)} w_i \delta(\vec{r} - \vec{r}_i), \tag{7}$$

where $I(m)$ is the number of collision or absorption events in the m-th stationary cycle, $\vec{r}_i$ is the position vector of these events and w_i is the statistical weight of a fission event at $\vec{r}_i$. The k_{eff} estimate at the m-th stationary cycle is then

$$\hat{k}^{(m)} = \frac{1}{N}\int \hat{S}^{(m)}(\vec{r})dr. \tag{8}$$

Eqs. (7) and (8) are equivalent to employing the fission site generation scheme and Keff estimator of a collision or absorption type. Eqs. (2), (5), (6) and (8) imply

$$k \equiv E[\hat{k}^{(m)}] = k_0 + \mathrm{O}(N^{-1}), \tag{9}$$

where $\equiv$ is used to imply the stationarity assumption.

The expected value (ensemble average) of the normalized source conditional on $\hat{S}^{(m-1)}(\vec{r})$ is written as

$$\frac{N\hat{S}^{(m-1)}(\vec{r})}{\int \hat{S}^{(m-1)}(\vec{r}')dr'}.$$

Then, the random noise component $\hat{\varepsilon}^{(m)}(\vec{r})$ resulting from the starter selection and subsequent particle tracking can be introduced as

$$\sqrt{N}\hat{\varepsilon}^{(m)}(\vec{r}) \equiv \hat{S}^{(m)}(\vec{r}) - \frac{N\int F(\vec{r}' \to \vec{r})\hat{S}^{(m-1)}(\vec{r}')dr'}{\int \hat{S}^{(m-1)}(\vec{r}'')dr''}. \tag{10}$$

As is shown in previous work[2], Eqs. (4) and (10) yield

$$\hat{e}^{(m)}(\vec{r}) = \int A(\vec{r}' \to \vec{r})\hat{e}^{(m-1)}(\vec{r}')dr' + \hat{\varepsilon}^{(m)}(\vec{r}) + O(N^{-1/2}), \tag{11}$$

where A is defined as

$$A(\vec{r}' \to \vec{r}) \equiv \frac{1}{k}F(\vec{r}' \to \vec{r}) - \frac{1}{k^2}\int F(\vec{q} \to \vec{r})S(\vec{q})dq. \tag{12}$$

The kernel A is rewritten, using (1), (6) and (9), as

$$A(\vec{r}' \to \vec{r}) = A_0(\vec{r}' \to \vec{r}) + O\left(N^{-1}\right), \tag{13}$$

where A_0 is defined to be

$$A_0(\vec{r}' \to \vec{r}) \equiv \frac{1}{k_0}\left[F(\vec{r}' \to \vec{r}) - S_0(\vec{r})\right]. \tag{14}$$

Eq. (11) then becomes

$$\hat{e}^{(m)}(\vec{r}) = \int A_0(\vec{r}' \to \vec{r})\hat{e}^{(m-1)}(\vec{r}')dr' + \hat{\varepsilon}^{(m)}(\vec{r}) + O(N^{-1/2}). \tag{15}$$

The operator notation of Eq. (15) may be introduced as

$$\hat{e}^{(m)} = A_0 \hat{e}^{(m-1)} + \hat{\varepsilon}^{(m)} + \mathrm{O}(N^{-1/2}), \tag{16}$$

The repeated application of Eq. (16) yields

$$\hat{e}^{(m)} = \sum_{j=0}^{m-1} A_0^j \hat{\varepsilon}^{(m-j)} + A_0^m \hat{e}^{(0)} + \mathrm{O}(N^{-1/2}). \tag{17}$$

To proceed further, we need two lemmas about $\hat{e}$'s and $\hat{\varepsilon}$'s. The first one is a result obtained in previous work[2]:

$$E[\hat{\varepsilon}^{(p)} \hat{e}^{(q)}] = 0, \; p > q. \tag{18}$$

Using this, one obtains the second lemma

$$\begin{aligned} E[\hat{\varepsilon}^{(p)} \hat{\varepsilon}^{(q)}] &= E[E[\hat{\varepsilon}^{(p)} \hat{\varepsilon}^{(q)} \mid \hat{e}^{(q)}, \hat{e}^{(q-1)}]] \\ &= E[\hat{\varepsilon}^{(q)} E[\hat{\varepsilon}^{(p)} \mid \hat{e}^{(q)}, \hat{e}^{(q-1)}]] \\ &= E[\hat{\varepsilon}^{(q)} E[\hat{\varepsilon}^{(p)} \mid \hat{e}^{(q)}]] \\ &= 0, \; p > q, \end{aligned} \tag{19}$$

where the vertical bar stands for conditioning on the accompanied quantities, the second equality is due to the fact that the conditioning on $\hat{e}^{(q)}$ and $\hat{e}^{(q-1)}$ is equivalent to the conditioning on $\hat{S}^{(q)}$ and $\hat{S}^{(q-1)}$ by (4), under which $\hat{\varepsilon}^{(q)}$ is a fixed function by (10), and the third equality due to the Markovity in a sense that the conditioning on $\hat{S}$'s, i.e., $\hat{e}$'s, depends on only the most recent previous cycle. Since the operation of taking expectation is equivalent to the integral by a probability measure, one may change the order of integrals in the following manner:

$$E[A_0^p \hat{\varepsilon}^{(i)}(\vec{r}) A_0^q \hat{\varepsilon}^{(j)}(\vec{r}')] = A_0^p (A_0^q)' E[\hat{\varepsilon}^{(i)}(\vec{r}) \hat{\varepsilon}^{(j)}(\vec{r}')],$$

$$E[A_0^p \hat{\varepsilon}^{(i)}(\vec{r}) A_0^q \hat{e}^{(0)}(\vec{r}')] = A_0^p (A_0^q)' E[\hat{\varepsilon}^{(i)}(\vec{r}) \hat{e}^{(0)}(\vec{r}')],$$

where the prime in $(A_0^q)'$ stands for the operation on $\hat{\varepsilon}^{(j)}(\vec{r}')$. Thus, Eqs. (17), (18) and (19) yield

$$C_S(i) \equiv E[\hat{e}^{(m+i)}(\vec{r})\hat{e}^{(m)}(\vec{r}')] = \sum_{j=0}^{m-1} E[A_0^{i+j}\hat{\varepsilon}^{(m-j)}(\vec{r})A_0^j\hat{\varepsilon}^{(m-j)}(\vec{r}')] + E[A_0^{m+i}\hat{e}^{(0)}(\vec{r})A_0^m\hat{e}^{(0)}(\vec{r}')] + O(N^{-1/2}), \quad (20)$$

where the stationarity assumption is implied in the usage of $\equiv$. The integration of (20) yields

$$\begin{aligned} C_k(i) &\equiv E\{[\hat{k}^{(m+i)} - E(\hat{k}^{(m+i)})][\hat{k}^{(m)} - E(\hat{k}^{(m)})]\} \\ &= \frac{1}{N} E[\int\int \hat{e}^{(m+i)}(\vec{r})\hat{e}^{(m)}(\vec{r}')drdr'] \\ &= \frac{1}{N}\sum_{j=0}^{m-1} E\left[\int A_0^{i+j}\hat{\varepsilon}^{(m-j)}(\vec{r})dr \int A_0^j\hat{\varepsilon}^{(m-j)}(\vec{r}')dr'\right] + \frac{1}{N} E\left[\int A_0^{i+m}\hat{e}^{(0)}(\vec{r})dr \int A_0^m\hat{e}^{(0)}(\vec{r}')dr'\right] \\ &\quad + \mathrm{O}(N^{-3/2}). \end{aligned} \quad (21)$$

Eqs. (20) and (21) imply that the decay of the autocorrelation of sources and k_{eff} tallies depends on how fast or slow $A_0^i S_j,\ j = 0,1,\ldots$ decays as i increases if the completeness assumption of S_j's is valid:

$$\hat{\varepsilon}^{(p)}(r) = \sum_{j=0}^{\infty} s_j^p S_j(\vec{r}) \text{ and } \hat{e}^{(0)}(r) = \sum_{j=0}^{\infty} s_j^0 S_j(\vec{r}). \quad (22)$$

Obviously, it is of considerable importance to know precisely what are the restrictions on the arbitrariness of the function to be expanded by S_j's. However, we simply approximate the Dirac delta function $\delta(\vec{r} - \vec{r}_l)$ appearing in the explicit form of $\hat{e}$'s and $\hat{\varepsilon}$'s by a function like

$$\delta(\vec{r} - \vec{r}_l) \approx \eta(\vec{r}) = \begin{cases} 1/(2\Delta)^3 & \vec{r} \in (r_{l,x} - \Delta, r_{l,x} + \Delta)(r_{l,y} - \Delta, r_{l,y} + \Delta)(r_{l,z} - \Delta, r_{l,z} + \Delta) \\ 0 & \text{otherwise} \end{cases}, \quad (23)$$

where Δ is a number as small as machine precision. We then assume the completeness of S_j's in L^2 space. Note that the above completeness assumption is valid for energy independent problems because $F(\vec{r}' \to \vec{r})$ is self-adjoint (Hermitian).[6]

Now, with the expansion in (22), one can focus on how S_j's are mapped by A_0. From Eqs. (1), (2) and (14), one immediately obtains

$$A_0 S_0(\vec{r}) = 0 . \tag{24}$$

This is a mathematical representation of the fact that a statistical error consisting of only the fundamental mode can be eliminated by source normalization. Eqs. (1) and (14) also yield

$$A_0 S_j(\vec{r}) = \frac{k_j}{k_0} S_j(\vec{r}) - \frac{\int S_j(\vec{r})dr}{k_0} S_0(\vec{r}) \quad j = 1,2,\ldots. \tag{25}$$

The repeated application of Eqs. (24) and (25) yields

$$A_0^i S_j(\vec{r}) = \left(\frac{k_j}{k_0}\right)^{i-1} \left[\frac{k_j}{k_0} S_j(\vec{r}) - \frac{\int S_j(\vec{r})dr}{k_0} S_0(\vec{r}) \right] \quad i, j = 1,2,\ldots. \tag{26}$$

Combining Eq. (26) with the normalization scheme (3), one obtains

$$A_0^i S_j(\vec{r}) = \begin{cases} \left(\frac{k_j}{k_0}\right)^i \left[S_j(\vec{r}) - S_0(\vec{r}) \right] & \text{when} \quad \int S_j(\vec{r})dr \neq 0 \\ \left(\frac{k_j}{k_0}\right)^i S_j(\vec{r}) & \text{when} \quad \int S_j(\vec{r})dr = 0 \end{cases}, \; j \geq 1. \tag{27}$$

Eqs. (20), (22), (24) and (27) imply that the autocorrelation of MC sources is largely influenced by the nonfundamental to fundamental mode eigenvalue ratios, especially the dominance ratio k_1/k_0. The integration of Eq. (27) over domain is combined with (3) to yield

$$\int A_0^{\,i} S_j(\vec{r})dr = \begin{cases} k_0 \left(\frac{k_j}{k_0}\right)^i \left(\frac{k_j}{k_0} - 1\right) & \text{when } \int S_j(\vec{r})dr \neq 0 \\ 0 & \text{when } \int S_j(\vec{r})dr = 0 \end{cases}, i \geq 1, \; j \geq 1. \tag{28}$$

Eqs. (21), (22) and (28) combined with Eq. (24) imply that the contribution of the fundamental mode to the autocorrelation of k_{eff} ($C_k(i),\ i \geq 1$) is zero and when the dominance ratio is close to unity, the contribution of the first mode to $C_k(i),\ i \geq 1$ is negligible. Therefore, $C_k(i),\ i \geq 1$, are small and may be negligible for problems with a dominance ratio close to unity. On the other hand, the integration of $A_0^{\,i} S_j$ over a subdomain yields:

$$\int_{subdomain} A_0^{\,i} S_j(\vec{r})dr = \begin{cases} \left(\frac{k_j}{k_0}\right)^i \int_{subdomain} \left[S_j(\vec{r}) - S_0(\vec{r})\right]dr & \text{when } \int S_j(\vec{r})dr \neq 0 \\ \left(\frac{k_j}{k_0}\right)^i \int_{subdomain} S_j(\vec{r})dr & \text{when } \int S_j(\vec{r})dr = 0 \end{cases}, \ j \geq 1, i \geq 1. \quad (29)$$

In general, Eq. (29) implies that the autocorrelation decay of the fission rate for subdomains is governed by the ratio of nonfundamental to fundamental mode eigenvalues, especially the dominance ratio. However, in symmetric systems, $\int_{subdomain} S_1(\vec{r})dr$ may vanish if the subdomain is symmetric with respect to the line or plane of the anti-symmetry of the first mode eigenfunction. The autocorrelation of the fission rate at such a subdomain decays faster than a factor of dominance ratio.

The derivation of an expression similar to Eq. (29) is not straightforward for flux tallies. However, flux tallies are expected to be largely influenced by the autocorrelation of sources because starters at each cycle are selected from the sources and there is no reason that a factor of (k_j/k_0−1) would appear in the autocorrelation analysis of flux tallies. Therefore, the summary of this section can be stated as follows: When the dominance ratio of a fission kernel is close to unity, the autocorrelation of Keff tallies is

weak and may be negligible, while the autocorrelation of local tallies such as the fission rate distribution is strong and decays slowly.

III. EXCLUSION OF INITIAL NONSTATIONARY TALLIES

It has been known for decades that MC source convergence is very slow for problems with a large dominance ratio if the shape of the guessed initial source departs from that of the stationary source, i.e., the fundamental mode. Recent work[7] showed that tallies contaminated by initial nonstationarity may yield erroneously overestimated autocorrelation. It is therefore necessary to take some means to diagnose the stationarity of the MC source distribution. To this end, we propose the posterior graphical diagnostics of the Shannon and relative entropies of source. First, Shannon entropy H is defined as follows[3]:

$$H(S^B) \equiv -\sum_{i=1}^{B} S^B(i) \ln(S^B(i)), \tag{30}$$

where B is the number of spatial bins, i the bin number and $S^B(i)$ a normalized binned source. H can be interpreted as a measure of randomness in the assumed resolution associated with a particular binning in the sense that H attains the maximum value $\ln(B)$ when $S^B = 1/B$ at all bins and the minimum value zero when $S^B = 1$ at one bin and $S^B = 0$ at all other bins. It should be noted that H assumes the same form as in the Boltzmann's H theorem. In information theory, the logarithm with base 2 is used instead of the natural logarithm, and $H(S^B)$ is the data compression limit of the random bins chosen from S^B.[8] In other words, Shannon entropy is directly related to another expression of randomness, i.e., the data compression limit. Thus, by computing H at each cycle, one can diagnose the source distribution in terms of randomness. In practice, we

make a one cycle delay-embedding plot of H borrowing an idea of delay reconstruction[9] in time series analysis methods. We plot the one cycle delay vector $\vec{H} \equiv [H(S^B, l), H(S^B, l+1)]$ where $H(S^B, l)$ denotes the Shannon entropy of the binned source S^B at the cycle l counted from the initial cycle. The trajectory of $\vec{H}$ through stationary cycles forms an equilibrium region from which $\vec{H}$'s in the initial nonstationary cycles may depart. The plotting of $\vec{H}$ can be utilized as a posterior visual diagnostic to identify the first cycle at which $\vec{H}$ enters the equilibrium region.

Second, the relative entropy (Kullback Leibler distance) of the normalized binned sources S^B and T^B with respect to S^B is defined as[3]

$$D(S^B \,||\, T^B) = \sum_{i=1}^{B} S^B(i) \ln\left(\frac{S^B(i)}{T^B(i)}\right).$$

$D(S^B||T^B)$ is a statistical distance between S^B and T^B in the sense that $D(S^B||T^B)$ is nonnegative and becomes zero only when $S^B(i) = T^B(i)$ for all bins. In addition, $D(S^B||T^B)$ satisfies the pair convexity

$$D(\lambda S_1^B + (1-\lambda)S_2^B \,||\, \lambda T_1^B + (1-\lambda)T_2^B) \le \lambda D(S_1^B \,||\, T_1^B) + (1-\lambda) D(S_2^B \,||\, T_2^B),\ 0 \le \lambda \le 1,$$

where S_1^B, S_2^B, T_1^B and T_2^B are all binned source normalized to unity.[8] Then, the S^B convexity follows by setting $T_1^B = T_2^B = T^B$:

$$D(\lambda S_1^B + (1-\lambda)S_2^B \,||\, T^B) \le \lambda D(S_1^B \,||\, T^B) + (1-\lambda) D(S_2^B \,||\, T^B),\ 0 \le \lambda \le 1.$$

This convexity relation is desired characteristics when one analyzes the statistical distance to the fixed reference source T^B. When $S^B \approx T^B$ for all bins, $D(S^B||T^B)$ is approximately equal to half of the χ-square distance:

$$D(S^B \,||\, T^B) = -\sum_{i=1}^{B} S^B(i) \ln\left[1 + \frac{T^B(i) - S^B(i)}{S^B(i)}\right]$$
$$= \frac{1}{2}\sum_{i=1}^{B} \frac{[T^B(i) - S^B(i)]^2}{S^B(i)} + \sum_{i=1}^{B} \mathrm{O}\left[\left(\frac{T^B(i) - S^B(i)}{S^B(i)}\right)^3\right],$$

where at the second equality $\sum_{i=1}^{B} S^B(i) = \sum_{i=1}^{B} T^B(i) = 1$ was used as well as the series expansion of $\log(1+x)$. Since $S^B(i)$ appears in denominators in the above expression and $D(S^B||T^B)$ is convex when viewed as a function of S^B, $D(S^B||T^B)$ can be interpreted as a measure of the inefficiency of assuming that the true distribution in a simulation is T^B when the observed distribution is S^B. Based on this interpretation, a posterior defensive visual diagnostic can be proposed as follows: After all cycles are simulated, 1) compute $T^B(i)$ by averaging source over the second half of active cycles from which k_{eff} tallies and other tallies of interest were collected, 2) plot $D(S^B||T^B)$ for each source S^B through cycles starting at the initial cycle, and 3) check whether $D(S^B||T^B)$ crosses the average of $D(S^B||T^B)$ over the second half of the active cycles before the first active cycle begins.

IV. NUMERICAL RESULTS

We numerically demonstrate what is implied in the analytical results in Section II. The first problem chosen to this end is an energy-independent infinite-slab version of loosely coupled two fissile component systems. The problem description is as follows:

Problem 1

- 5 region slab, with void boundary conditions on both sides and one-group isotropic cross sections,
- the regions are (left to right) 1.0, 1.0, 5.0, 1.0, and 1.01 cm thickness,

- the materials are (left to right) 2 (fuel), 1 (scatterer), 3 (absorber), 1, and 2,

- material 1 (scatterer)
$\Sigma_{total} = 1.0\, cm^{-1}, \Sigma_{scattering} = 0.8\, cm^{-1}, \Sigma_{capture} = 0.2\, cm^{-1}$,

- material 2 (fuel)
$\Sigma_{total} = 1.0\, cm^{-1}, \Sigma_{scattering} = 0.8\, cm^{-1}, \Sigma_{capture} = 0.1\, cm^{-1}, \Sigma_{fission} = 0.1\, cm^{-1}, \nu = 3.0$,

- material 3 (absorber)
$\Sigma_{total} = 1.0\, cm^{-1}, \Sigma_{scattering} = 0.1\, cm^{-1}, \Sigma_{capture} = 0.9\, cm^{-1}$.

The first six eigenvalues are computed to be 0.427425, 0.424221, 0.130633, 0.129265, 0.071924 and 0.071173 by Green's function method[10]; the dominance ratio is 0.993. The same dominance ratio value is also obtained by analyzing the spectral radius of the outer iterations in a discontinuous finite element discrete ordinate computation[11]. Figure 1 shows the autocorrelation coefficient (ACC) of k_{eff} and the source at the right fissile slab where simulation parameters are 50000 histories per cycle and 2000 active and 500 inactive cycles, the initial source is flat, and the standard deviations of ACC is computed by Bartlett's approximate formula assuming a normal (Gaussian) process[12]. It can be observed that the ACC of k_{eff} is nearly zero while the ACC of the source at the right fissile slab decays by about a factor of the dominance ratio. This confirms the analysis in Section II, especially what is implied in Eqs. (28) and (29). To check that the beginning of active cycles had been in stationarity, the methods in Section III were applied with one space bin assigned to each fissile slab. Figure 2 shows the one cycle delay embedding plot of the Shannon entropy of the source distribution. The delay vector is observed to have entered an equilibrium region before the active cycle begins at cycle 501. Figure 3 shows the relative entropy of the source distribution assuming that the true source is the mean source over the second half of active cycles. It is again observed that stationarity

was achieved before the beginning of active cycles. Therefore, one can conclude that the results in Figure 1 are not contaminated by initial nonstationarity.

To investigate the effect of symmetry on the autocorrelation of the fission rate at space bins, a homogeneous infinite square column system was chosen as the second problem. Figure 4 shows the problem description with space binning. The dominance ratio is computed to be 0.987 by the discontinuous finite element discrete ordinate method. The ACC of Keff, the source at the bin (12,12), and the combined bin (12,12)+(12,13)+(13,12)+(13,13) are shown in Figure 5 where simulation parameters are 100000 histories per cycle, 5000 active and 200 inactive cycles, flat initial source, and the standard deviation of ACC is again computed by Bartlett's formula. The above bin choices are based on the shape of the first to tenth mode eigenfunctions obtained by fission matrix analysis[13]. In Figure 4, one of the thick center lines is the line of anti-symmetry of the first and second mode eigenfunctions (Figures 6 and 7) in the sense that they assume values of the same magnitude with opposite signs at points symmetric to that line. Also, both of the thick center lines in Figure 4 are the line of anti-symmetry of the third mode eigenfunction (Figure 8) in the same sense. Therefore, the first to third mode eigenfunctions are anti-symmetric in the combined bin, but they are not inside the bin (12,12) alone. More precisely, the following relations hold:

$$
\begin{aligned}
0 &= \int_{(12,12)+(12,13)+(13,12)+(13,13)} S_1(\vec{r})dr \\
&= \int_{(12,12)+(12,13)+(13,12)+(13,13)} S_2(\vec{r})dr \\
&= \int_{(12,12)+(12,13)+(13,12)+(13,13)} S_3(\vec{r})dr,
\end{aligned}
$$

$$\int_{(12,12)} S_1(\vec{r})dr \neq 0,$$

$$\int_{(12,12)} S_2(\vec{r})dr \neq 0,$$

$$\int_{(12,12)} S_3(\vec{r})dr \neq 0.$$

It can be observed in Figure 5 that the ACC of Keff is negligible, the ACC of the source at the combined bin decays much faster than a factor of the dominance ratio and the ACC of the source at bin (12,12) decays by a factor of the dominance ratio for lags larger than ten. Actually, the ACC of source at bin (12,12) for 10 and 50 lags are 0.202 ± 0.034 and 0.108 ± 0.030 yielding their ratio of 0.54 ± 0.17, while the fortieth power of dominance ratio is $(0.987)^{40}$=0.593. On the other hand, the ACC of the source at the combined bin for 10 and 20 lags are 0.313 ± 0.033 and 0.124 ± 0.041 yielding their ratio of 0.40 ± 0.14, while the tenth power of dominance ratio is $(0.987)^{10}$=0.877. Here, we picked 10 and 20 lags because zero is contained in the 3σ confidence interval of the ACC at the combined bin for lags larger than 20. In addition, as discussed in the Appendix, both the ACCs pose a serious challenge in confidence interval estimation. The rough evaluation using inequality (A.6) shows that variance estimation bias is at least four times as large as sample variance for the source at these bins. Figure 9 shows the one cycle delay embedding plot of the Shannon entropy of the source. The delay vector is observed to have entered an equilibrium region before the active cycle begins at cycle 201. Figure 10 shows the relative entropy of the source assuming that the true source is the mean source over the second half of active cycles with the condition of 2000 active 200 inactive cycles. It is again observed that stationarity was achieved before the beginning of active cycles. In the actual computation, we continue another 3000 cycles to get more accuracy

in ACC estimation. The effect of dominance ratio on the ACC of the source at the lower left 2 cm $\times$ 2 cm bin adjacent to the center is shown in Figure 11 where the square size in Figure 4 is changed to 12 cm $\times$ 12 cm and 64 cm $\times$ 64 cm to yield a dominance ratio of 0.868 and 0.992, respectively. Here, these dominance ratio values were computed by the discontinuous finite element discrete ordinate method. It is observed that for the problem with a dominance ratio of 0.868, the ACC decays moderately, its value at lag 11 contains zero within a 3σ confidence interval, and its value at lags larger than 11 is fluctuating near zero, while for the problem with a dominance ratio of 0.992, the ACC decays by a factor slightly smaller than 0.992 and is at least 4σ away from zero. Before plotting Figure 11, the methods in Section III were used, as before, to confirm that stationarity was achieved before the first active cycle. We omit the results because they are similar to Figures 2, 3, 9 and 10.

The ACC of k_{eff} may become significant when the dominance ratio is $0.80 \sim 0.90$ because as indicated in Eq. (28), a factor of $\left(k_j / k_0\right)^i \left(k_j / k_0 - 1\right)$ dominates the whole domain integral of the i-times operation of the error propagation operator on the j-th eigenfunction. Recent work has shown that the sharp spatial variation of the immediate importance of source particles may introduce large bias in the sample variance estimator.[2] Therefore, we compare the homogeneous 24 cm $\times$ 24 cm problem with the cross sections in Figure 4 and a heterogeneous 24 cm $\times$ 24 cm problem with the same cross sections except the central 3 cm $\times$ 3 cm square; $\nu\Sigma_f = 0.24\, cm^{-1}$ is replaced by $\nu\Sigma_f = 0.39\, cm^{-1}$ in the central region. The dominance ratio is computed to be 0.954 for the homogeneous

problem and 0.846 for the heterogeneous problem by the discontinuous finite element discrete ordinate method. As shown in Figure 12, the ACC is observed to be negligible for the homogeneous problem, while it is significant for the heterogeneous problem. Using inequality (A.6) and the ACC at one to ten lags, the lower bound of variance estimation bias is computed to be 2.6 ± 0.2 times the expected value of sample variance for the heterogeneous problem, where correlation among ACCs at different lags is neglected in computing the standard deviation. Again, we omit the results of the stationarity check because they are similar to Figure 2, 3, 9 and 10.

V. CONCLUSION

We investigated the iteration cycle-to-cycle error propagation operator of MC stationary sources and derived mathematical expressions connecting the dominance ratio and eigenvalue ratios of a fission kernel to the autocorrelation of k_{eff} and fission source. What is implied in these expressions can be summarized as follows: When the dominance ratio of a fission kernel is close to unity, the autocorrelation of the tallies of k_{eff} is not strong and may be negligible, while the autocorrelation of the MC stationary sources is strong and decays slowly. This claim was numerically confirmed. Therefore, for criticality safety analysts, systems with large dominance ratio are only an issue of slow source convergence. However, for reactor analysts interested in the distribution of fission rate (power), systems with the dominance ratio close to unity may yield large bias in the sample variance estimator with no batch grouping and therefore pose a significant challenge in confidence interval estimation. The Shannon and relative entropies of the

source distribution were shown to be very useful in the posterior stationarity diagnostics of source.

APPENDIX: SIMPLE EVALUATION OF VARIANCE ESTIMATION BIAS

This appendix discusses variance estimation bias in terms of the sample variance with no batch grouping. To begin with, three notations are introduced:

σ_A^2="Expected value of the sample variance with no batch grouping for the average of stationary cycle tallies,"

σ_R^2="Variance of the average of stationary cycle tallies,"

C(i)="Lag *i* autocovariance of cycle tallies."

σ_A^2 and *C*(i) satisfy[14]

$$\sigma_A^2 = \frac{C(0)}{M} - \frac{2}{M^2(M-1)} \sum_{i=1}^{M-1} (M-i)C(i), \tag{A.1}$$

where *M* is the number of stationary cycles simulated. Eq. (A.1) immediately yields

$$0 \le \sigma_A^2 \le \frac{C(0)}{M} \quad \text{when} \quad C(i) \ge 0, i = 0, \ldots, M-1. \tag{A.2}$$

Also, σ_A^2, σ_R^2 and *C*(*i*) satisfy[14]

$$\sigma_A^2 - \sigma_R^2 = -\frac{2}{M(M-1)} \sum_{i=1}^{M-1} (M-i)C(i), \tag{A.3}$$

which immediately yields

$$0 \le \frac{2C(1)}{M} \le \sigma_R^2 - \sigma_A^2 \text{ if } C(i) \ge 0, i = 0, \ldots, M-1. \tag{A.4}$$

Inequalities (A.2) and (A.4) combined imply

$$0 \le \sigma_A^2 \le \sigma_R^2 - \sigma_A^2 \quad \text{when } C(1)/C(0) \ge 0.5 \text{ and } C(i) \ge 0, i = 0, \ldots, M-1. \tag{A.5}$$

Therefore, problems with a lag 1 autocorrelation coefficient of moderate magnitude have large variance estimation bias. Furthermore, (A.2) and (A.3) combined yield

$$\sigma_R^2 - \sigma_A^2 \geq 2\sigma_A^2 \left[\frac{C(1)}{C(0)} + \cdots + \frac{(M-i)C(i)}{(M-1)C(0)} + \sum_{j=i+1}^{M-1} \frac{M-j}{M-1} \frac{C(j)}{C(0)} \right] \quad \text{(A.6)}$$
$$\text{if } C(k) \geq 0, k = 0, \ldots, M-1.$$

This inequality implies that if autocorrelation coefficients have a moderate value for lags smaller than or equal to i $(\ll M)$ and decay slowly for lags larger than i, the variance estimation bias can become extremely large, which poses significant challenge on confidence interval estimation.

REFERENCES

1. D.B. MacMillan, "Monte Carlo Confidence limits for Iterated Source Calculations," *Nucl. Sci. Eng*., **50**, 73 (1973).
2. T. Ueki, "Intergenerational Correlation in Monte Carlo K-Eigenvalue Calculation," *Nucl. Sci. Eng*., **141**, 101 (2002).
3. R.S. Ellis, *Entropy, Large Deviations and Statistical Mechanics*, Springer-Verlag, New York (1985).
4. R.J. Brissenden and A.R. Garlick, "Biases in the Estimation of Keff and its Error by Monte Carlo Methods," *Ann. Nucl. Energy*, **13**, 2, 63 (1986).
5. T.M. Sutton and F.B. Brown, "Analysis of the Monte Carlo Eigenvalue Bias," (unpublished).
6. J.A. Cochran, *The Analysis of Linear Integral Equations*, McGraw-Hill, New York (1972).

7. T. Ueki and F.B. Brown, "Stationarity Diagnostics Using Shannon Entropy in Monte Carlo Criticality Calculation I: F test," ANS 2002 winter meeting, accepted. Also published as LA-UR-02-3783.
8. T.M. Cover and J.A. Thomas, *Elements of Information Theory*, John Wiley & Sons, New York (1991).
9. H. Kantz and T. Schreiber, *Nonlinear Time Series Analysis*, Cambridge University Press, Cambridge UK (1997).
10. D.E. Kornreigh and B.D. Ganapol, "The Green's Function Method for Nuclear Engineering Applications," *Nucl. Sci. Eng.*, **126**, 293 (1997).
11. T.A. Wareing, J.M. McGhee, J.E. Morel and S.D. Pautz, "Discontinuous Finite Element S_N Methods on Three-Dimensional Unstructured Grids," *Nucl. Sci. Eng.*, **138**, 256 (2001).
12. M.S. Bartlett, "On the theoretical specification and sampling properties of autocorrelated time-series," *J. Roy. Statist. Soc.*, **B8**, 27 (1946).
13. R.E. Alcouffe, R.S. Baker, F.W. Brinkley, D.R. Marr, R.D. O'Dell and W.F. Walters, "DANTSYS: A Diffusion Accelerated Neutral Particle Transport Code System, Los Alamos National Laboratory," LA-12969-M (1995).
14. T. Ueki, T. Mori and M. Nakagawa, "Error Estimations and Their Biases in Monte Carlo Eigenvalue Calculations," *Nucl. Sci. Eng.*, **125**, 1 (1997).

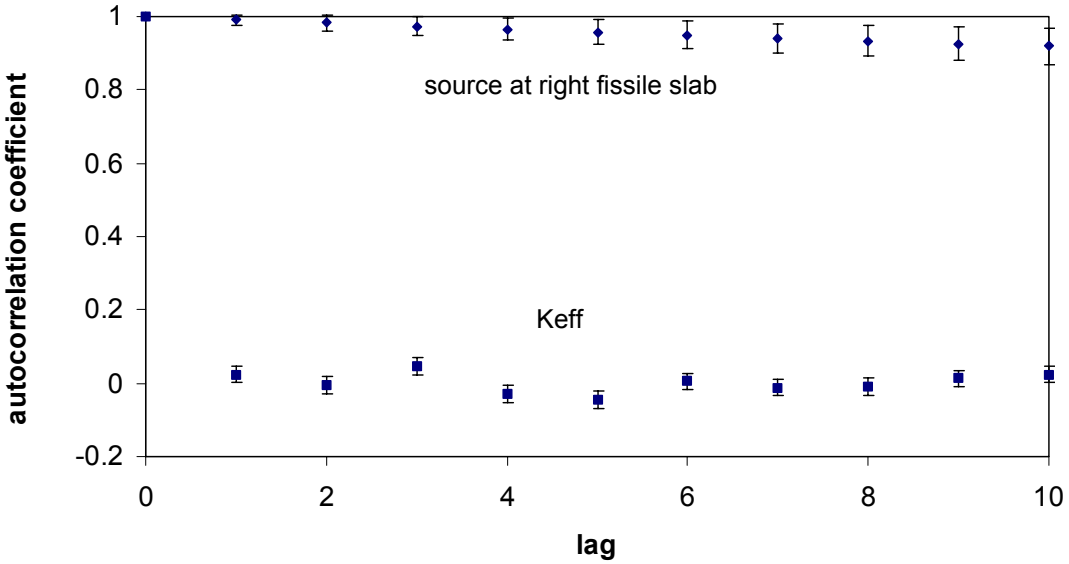

Figure 1: Autocorrelation versus cycle lag for problem 1 (2000 active and 500 inacive cycles with 50000 histories per cycle)

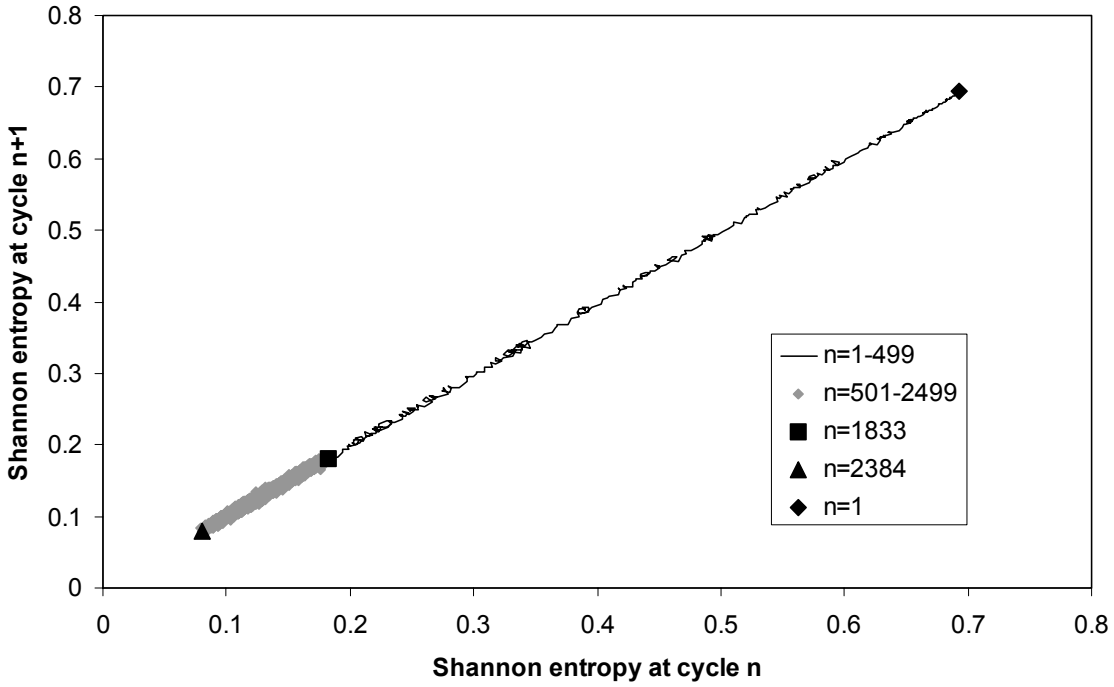

Figure 2: One cycle delay embedding plot of Shannon entropy of source (problem 1)

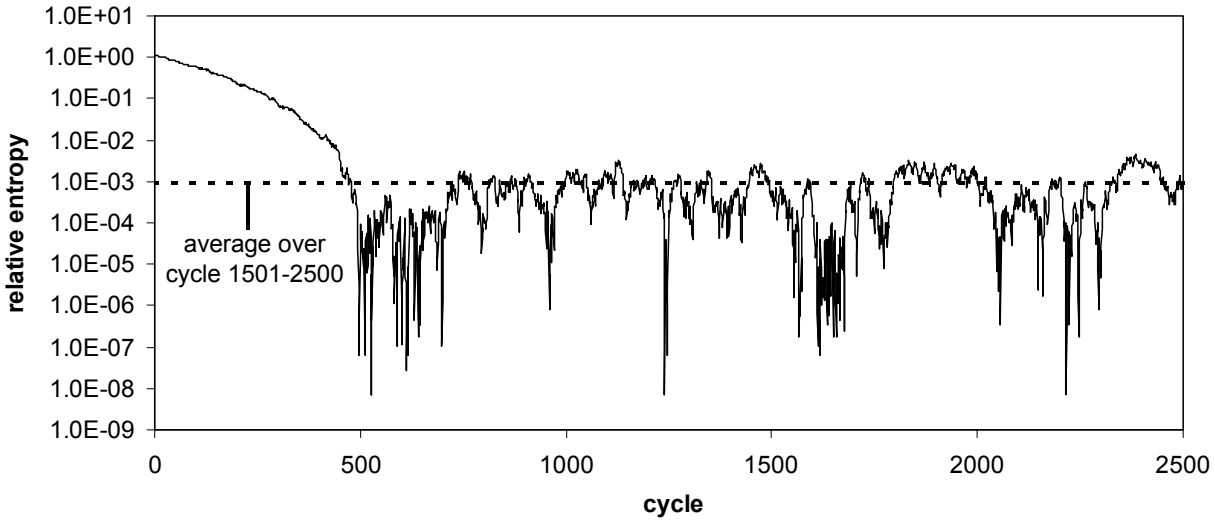

Figure 3: Posterior computation of relative entropy assuming the true source is the mean source over 1501-2500 cycles (problem 1)

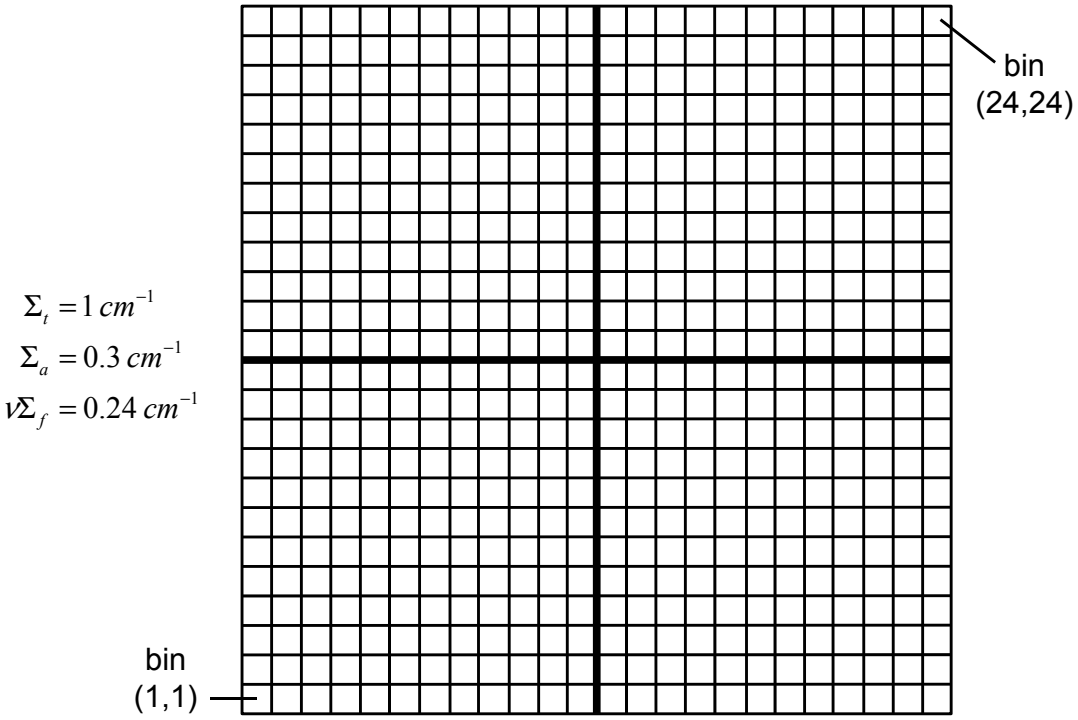

Figure 4: Uniform space binning for problem 2, 48 cm × 48 cm homogeneous infinite square column with vacuum boundary condition

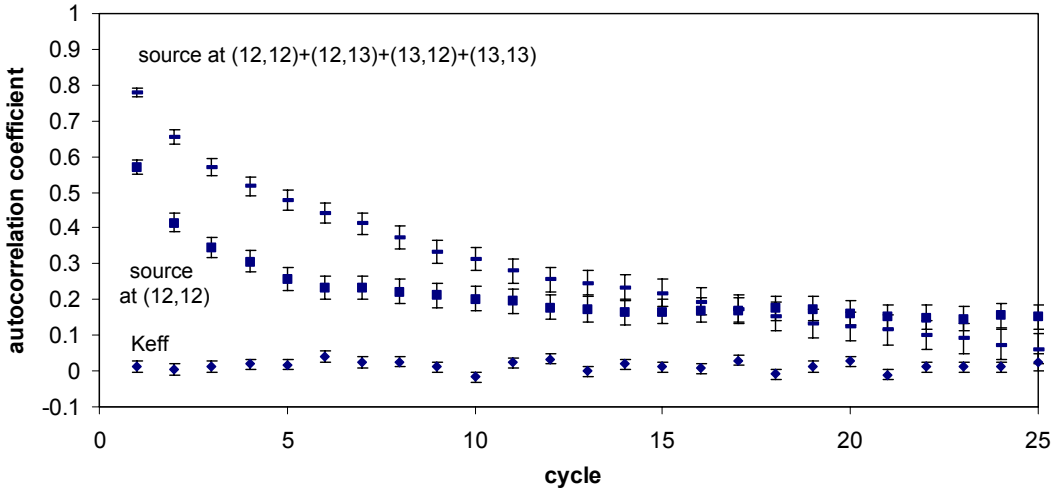

Figure 5: Autocorrelation versus cycle lag for problem 2, homogeneous 48 cm x 48 cm square (100000 histories per cycle, 5000 active and 200 inactive cycles)

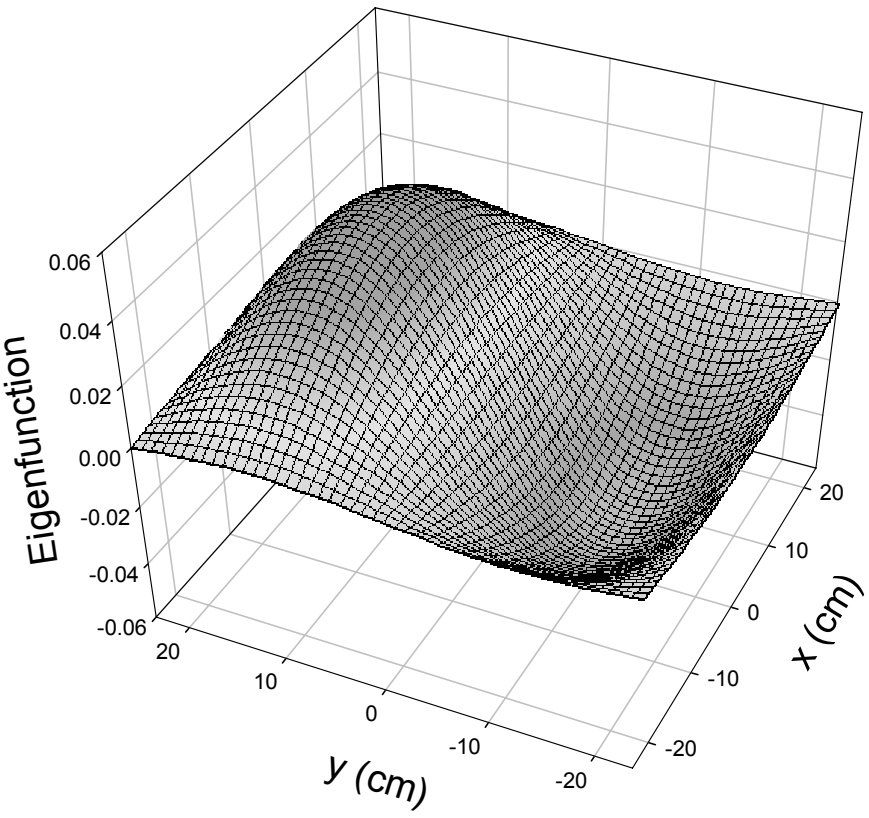

Figure 6: First mode eigenfunction for problem 2; first to fundamental mode eigenvalue ratio (dominance ratio) =0.987 (TWODANT-based fission matrix analysis)

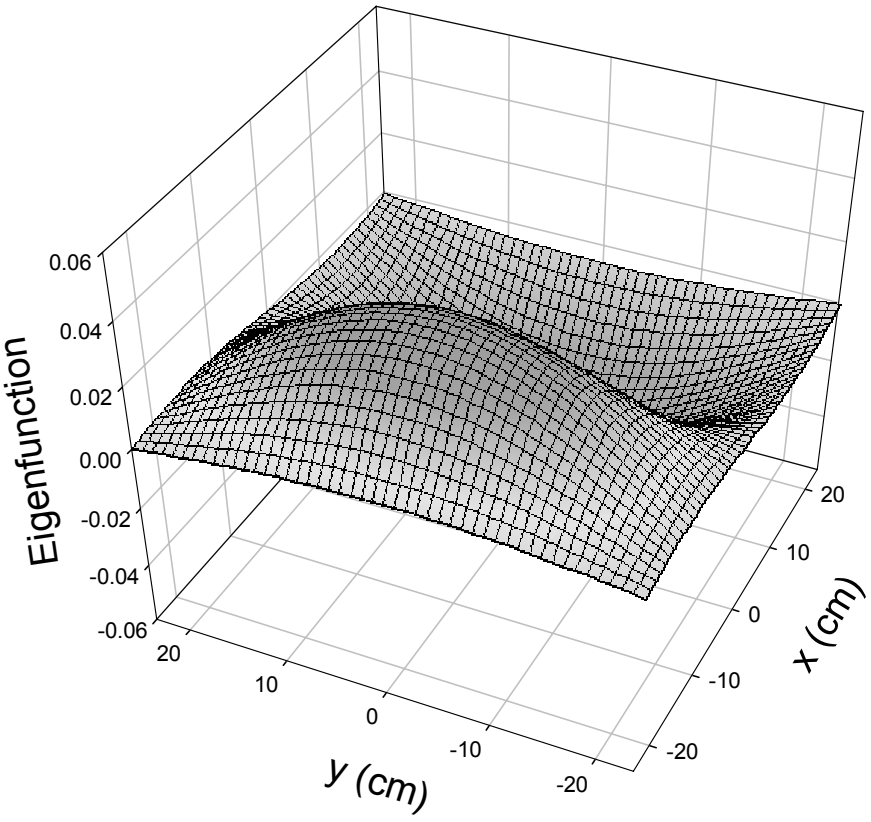

Figure 7: Second mode eigenfunction for problem 2; second to fundamental mode eigenvalue ratio =0.987 (TWODANT-based fission matrix analysis)

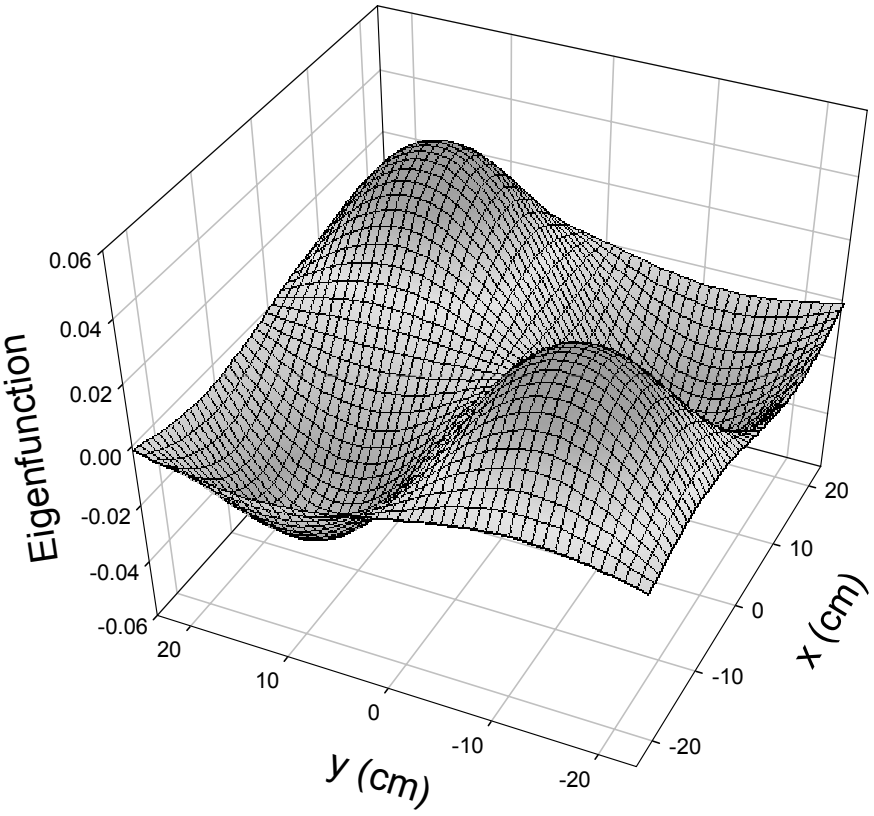

Figure 8: Third mode eigenfunction for problem 2; third to fundamental mode eigenvalue ratio =0.973 (TWODANT-based fission matrix analysis)

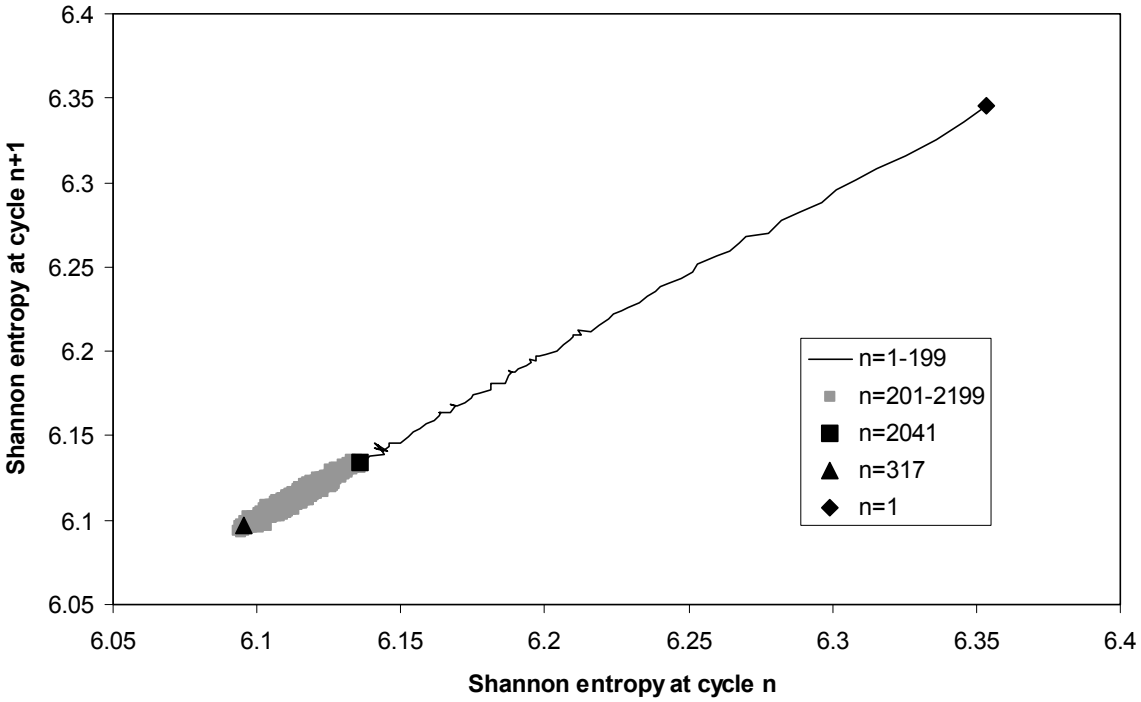

Figure 9: One cycle delay embedding plot of Shannon entropy of source (problem 2)

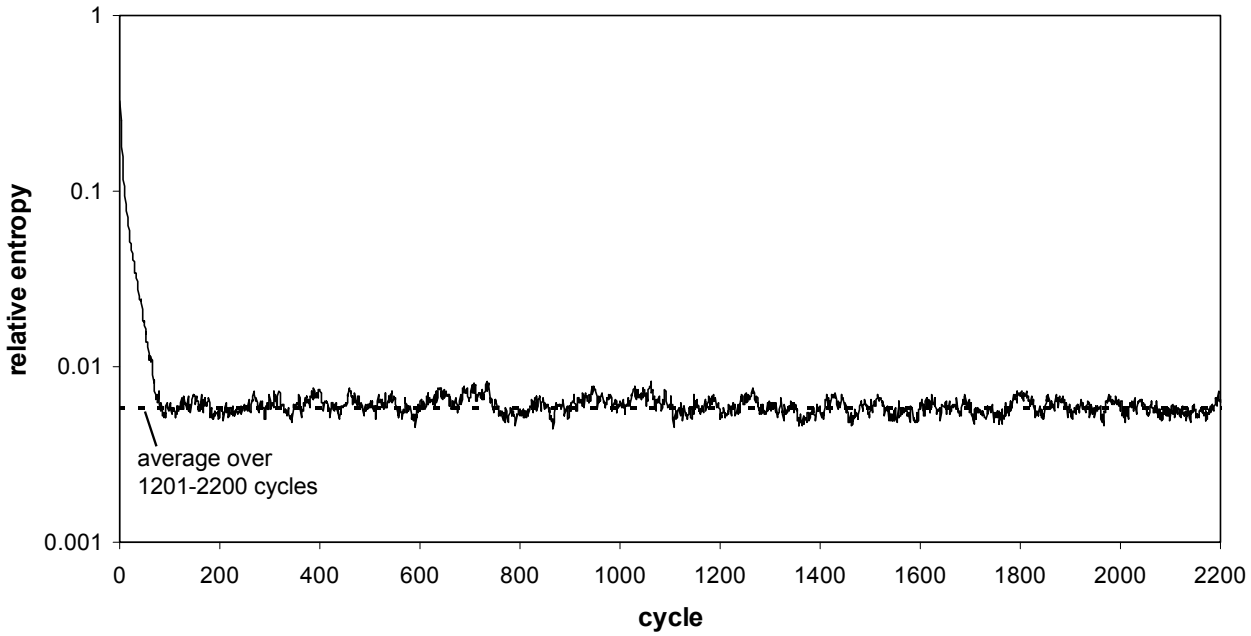

Figure 10: Posterior computation of relative entropy assuming the true source is the mean source over 1201-2200 cycles (problem 2)

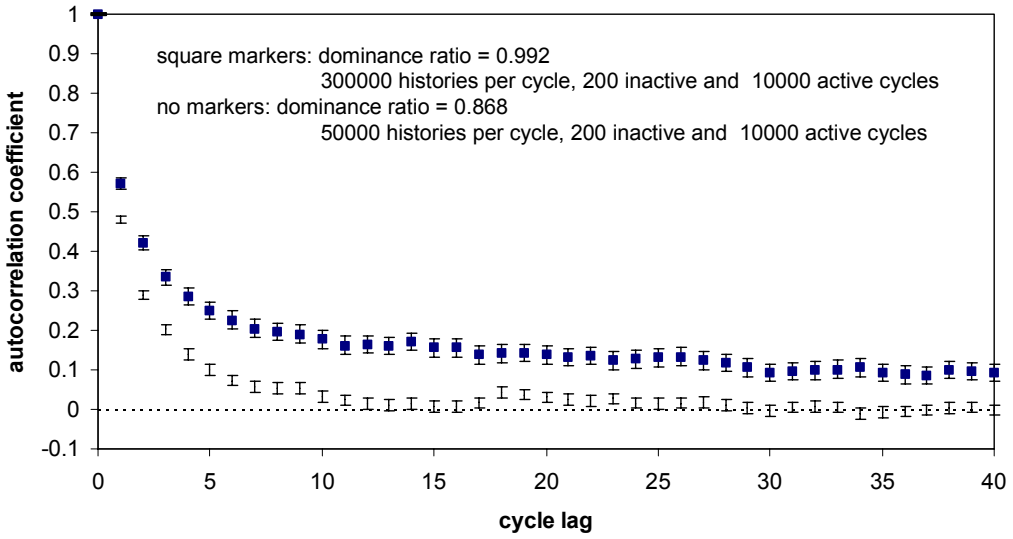

Figure 11: Effect of dominance ratio on autocorrelation of source at lower left bin adjacent to center for 2D homogeneous problem

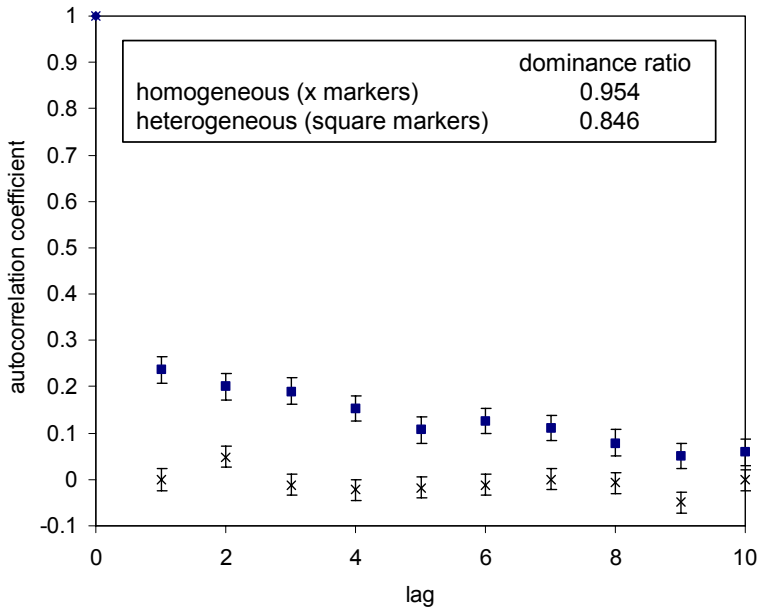

Figure 12: Autocorrelation of k_{eff} for 24 cm x 24 cm homogeneous and heterogeneous problems computed from 2200 active and 200 inactive cycles with 50000 histories per cycle